Nonlinear σ model and static holes

Khalil Bitar
Supercomputer Computations Research Institute, Florida State University, Tallahassee, Florida 32306

Efstratios Manousakis
Department of Physics,
Center for Materials Research and Technology and Supercomputer Computations Research Institute,
Florida State University, Tallahassee, Florida 32306

(Received 7 August 1990)

We study certain aspects of the nonlinear σ model regularized on the lattice in two space and one Euclidean-time dimensions using the Monte Carlo method. For certain purposes this model is considered as the long-wavelength limit of the quantum spin-S antiferromagnetic Heisenberg model in two space dimensions, where the different spin cases map to different values of the coupling constant g of the σ model. For the value of g that corresponds to the spin-$\frac{1}{2}$ case on the square lattice, we find that the most probable configurations are characterized by large-amplitude short-range quantum fluctuations. Such configurations lack smoothness, which, however, can be achieved by means of real-space block-spin transformations. We calculate the Berry phase correlations, namely, the correlation function $C_{ij} \equiv \langle \exp\{iS[\Sigma(\mathbf{r}_i) + (-1)^{|i-j|}\Sigma(\mathbf{r}_j)]\}\rangle$, where $\Sigma(\mathbf{r}_i)$ is the area on the unit sphere defined by the path of the spin located at the spatial lattice point $\mathbf{r}_i$ during its Euclidean-time evolution. We find that the contribution to hole-hole attraction from such correlations is limited to distances of a few lattice spacings. Finally, we examine the possible presence of topological monopole singularities in configurations, and we find only spin-wave excitations.

I. INTRODUCTION

The observation of long-range two-dimensional antiferromagnetic correlations[1] between electronic spins in the copper-oxide-based superconducting materials has generated ideas for a new type of pairing mechanisms. Furthermore, a recent analysis[2] of the NMR experiments suggests the existence of an antiferromagnetically correlated one-component Fermi liquid in the normal state. In the superconducting phase this liquid should transform, via an as-yet-not-understood mechanism, to a quantum liquid responsible for the superconductivity in these materials. The low-energy excitations of the undoped antiferromagnetic insulator La_2CuO_4 (the material that becomes metallic and superconducting upon doping), as seen by neutron- and Raman-scattering experiments, are spin-wave excitations whose spectrum and the behavior of spin correlations that they induce are accurately understood in terms of a spin-$\frac{1}{2}$ antiferromagnetic Heisenberg model (AFHM) on the square lattice[3]

$$\hat{H} = J \sum_{\langle i,j \rangle} \mathbf{S}_i \cdot \mathbf{S}_j \ , \tag{1}$$

using a value for the antiferromagnetic coupling $J \simeq 1500$ K.

Doping the antiferromagnetic insulator creates holes, and it has been suggested, based on the nature of such materials, that the dymamics could be described by adding to the Hamiltonian (1) hole-hopping terms such as $T = -t \sum_{\langle ij,\sigma \rangle} (c^{\dagger}_{i,\sigma} c_{j,\sigma} + \text{H.c.})$, where $c_{i,\sigma}$ is a hole creation operator. The strong on-site Coulomb repulsion is taken into account by restricting the action of the resulting Hamiltonian operator (known as the t-J model) in a subspace of the Hilbert space having states with singly occupied sites. Such models can arise naturally as the strong-correlation limit of the single-band Hubbard model or more realistic models that take into account the detailed chemical structure of the copper oxide planes.[4]

The quantum nonlinear σ model (QNLσM) in two space and one Euclidean-time dimensions can be derived as the long-wavelength limit of the spin-S antiferromagnetic Heisenberg model in two space dimensions under certain assumptions.[5,6] The QNLσM was first used to describe the spin-spin correlations in undoped La_2CuO_4 by Chakravarty, Halperin, and Nelson[7,8] using the momentum-space renormalization-group approach to calculate the temperature dependence of the correlation length. They suggested that the spin-$\frac{1}{2}$ AFHM at T=0 corresponds to the ordered phase of the QNLσM and that the correlation length behaves as

$$\xi(T \to 0) = C e^{\frac{2\pi\rho_s}{T}} \ . \tag{2}$$

Later, Manousakis, and Salvador[9] studied the QNLσM using lattice regularization and Monte Carlo simulation. They found that the correlation length in the ordered phase behaves as given by Eq. (2); by making contact with the simulation of the spin-$\frac{1}{2}$ AFHM, they obtained the spin-stiffness constant $\rho_s \simeq 0.2J$. Using this behavior

the neutron-scattering data for the correlation length fit accurately[3] with $J \simeq 1500$ K.

In this paper, we study certain other aspects of the QNLσM using lattice regularization and Monte Carlo simulation, as in Ref. 9. First, we examine the smoothness of the configurations and the paths on the unit sphere during their Euclidean-time evolution. For the value of the coupling constant g of the σ model that corresponds to the spin-$\frac{1}{2}$ case on the square lattice, we find that the configurations lack smoothness, due to large-amplitude short-range fluctuations. However, smoothness occurs only after block-spin transformations where we recover the long-distance correlations. Our results and discussion about such questions are presented in Sec. III.

Shankar[10] has recently suggested that holes introduced in the σ model when they are on different (the same) sublattices behave as charges with opposite (the same) charge. The hole, in his formalism, couples to the spin degrees of freedom through a gauge field due to coherent interference between the Berry phases, which the spins would have contributed if they were there at the hole positions. A static potential, in this approach, can be numerically calculated by calculating the correlation function $C_{ij} \equiv \langle \exp\{iS[\Sigma(\mathbf{r}_i) + (-1)^{|i-j|}\Sigma(\mathbf{r}_j)]\}\rangle$, where $\Sigma(\mathbf{r}_i)$ is the area on the unit sphere defined by the path of the spin located at the spatial lattice point $\mathbf{r}_i$ during its Euclidean-time evolution. We find that the contribution to hole-hole attraction from such correlations is limited to distances of a few lattice spacings.

Finally, in Sec. V we examine the possible role that topological monopole configurations might play. In the ordered phase, starting from a random configuration it takes many sweeps to reach thermalization; away from equilibrium, we have observed smooth configurations with rich structure. We calculated the net monopole charge inside a cube of variable size for such configurations, and we concluded that the structures have no monopole charge distribution. The smooth fluctuations are only large-amplitude spin-wave excitations that do not cover the unit sphere to give rise to a nontrivial topological charge. We conclude that in the ordered phase of the σ model only spin-wave excitations are present in 2+1 dimensions.

II. FORMULATION AND NONLINEAR σ MODEL

Let us start by giving an outline of the derivation of the path-integral representation of the partition function of the antiferromagnetic Heisenberg model using coherent states for spins. More detailed derivation has been given in other papers including the review paper of Ref. 3. Here we repeat the main steps for easy reference and because we shall discuss certain aspects related to the derivation. From this representation we can pass to the continuum limit where the quantum-mechanical nonlinear σ model is obtained as a model that describes smooth spin configurations. In this formulation, the state of a spin at a given site is expressed in the following coherent basis:

$$|\Omega\rangle \equiv |\theta,\phi\rangle \equiv e^{-i\phi(\hat{S}_z - S)} e^{-i\theta \hat{S}_y} |S\rangle \ , \tag{3}$$

where Ω is a vector on the unit sphere with spherical coordinates $(1,\theta,\phi)$, $0 \le \theta < \pi$ and $0 \le \phi < 2\pi$ and the state $|S>$ is the eigenstate of $\hat{S}_z$ with the largest possible eigenvalue S. Note that this definition establishes a correspondence between coherent states and points on the unit sphere. The basis (3) is overcomplete and the overlap between such states can be easily calculated to give

$$\langle \Omega' | \Omega \rangle = \left(\cos\frac{\theta}{2}\cos\frac{\theta'}{2} + e^{-i(\phi'-\phi)} \sin\frac{\theta}{2}\sin\frac{\theta'}{2} \right)^{2S} \ . \tag{4}$$

It can be verified that

$$\langle \Omega' | \Omega \rangle = |\langle \Omega' | \Omega \rangle| e^{-i\Phi} \ , \tag{5}$$

$$|\langle \Omega' | \Omega \rangle| = [\tfrac{1}{2}(1 + \Omega' \cdot \Omega)]^S \ . \tag{6}$$

Assuming smooth paths in imaginary time, i.e., that the vectors Ω and Ω' are close, we obtain

$$\Phi = (1 - \cos\theta)\Delta\phi + \cdots \ , \tag{7}$$

where the dots stand for higher-order terms in $\Delta\phi$ and $\Delta\theta$. Notice that Φ coincides with the area of the spherical triangle formed by the north pole and the tips of the unit vectors Ω and Ω'. Inserting the resolution of the identity operator $I = \int d\Omega/4\pi |\Omega\rangle\langle\Omega|$ at each site and writing $e^{-\beta\hat{H}} = \prod_{i=1}^{M}(1 - \epsilon\hat{H})$, with $\beta = M\epsilon$, the partition function Z takes the following form:

$$Z = \int [D\Omega] \prod_{i=1}^{M} \langle \Omega_1(\tau_i + \epsilon) \cdots \Omega_N(\tau_i + \epsilon) | 1 - \epsilon\hat{H} | \Omega_1(\tau_i) \cdots \Omega_N(\tau_i) \rangle \ . \tag{8}$$

The real part of the overlap between neighboring (in time) coherent states is $|\langle \Omega' | \Omega \rangle| = \exp[S \ln(1 - \frac{1}{4}|\Omega' - \Omega|^2)] \simeq \exp[-(S/4)(\partial\Omega/\partial\tau)^2\epsilon^2]$ and may be approximated by 1, and the corrections are of order ϵ^2. Furthermore, it is straightforward to show that $\langle \Omega | \mathbf{S} | \Omega \rangle = S\Omega$, from which it follows that

$$H \equiv \langle \{\Omega_i\} | \hat{H} | \{\Omega_i\} \rangle = S^2 J \sum_{(ij)} \Omega_i \cdot \Omega_j \ . \tag{9}$$

Hence the partition function is given by

$$Z = \int [D\Omega] \exp\left(-iS \int_0^\beta (1 - \cos\theta) d\phi - S^2 J \int_0^\beta \sum_{(ij)} \Omega_i \cdot \Omega_j d\tau \right) \ . \tag{10}$$

The first term is the total solid angle α_i, which is the area of the closed trajectory of the vector $\Omega_i(\tau)$ characterizing the state of the ith spin to start and end up at the same point at $\tau = \beta$. Using Stokes' theorem the area on the sphere can be written as $\int\int \Omega \cdot \Omega \, d\sigma = \oint \mathbf{A} \cdot d\Omega$ where $d\sigma$ is the surface element of the sphere and the vector potential $\mathbf{A}$ is given as a solution to the following equation: $\nabla_{\Omega} \times \mathbf{A}(\Omega) = \Omega$. The vector potential $\vec{A}(\vec{\Omega})$ is known up to a gauge transformation $\mathbf{A} \rightarrow \mathbf{A} + \nabla_{\Omega}\lambda$. The phase factor, $iS\alpha_i$, is also known as the Berry phase for the adiabatic motion of a quantum spin.

Haldane[6] has derived a continuum field theory of the two-dimensional (2D) Heisenberg antiferromagnet using the coherent spin-basis representation as follows. In an antiferromagnet, *smooth* paths can be written as combination of two fields

$$\Omega_i(\tau) \simeq (-1)^{||\mathbf{r}_i||} \sqrt{1 - \left(\frac{a^d \mathbf{L}_i(\tau)}{S}\right)^2} \, \mathbf{n}_i(\tau) + \frac{a^d}{S} \mathbf{L}_i(\tau) \, , \tag{11}$$

where $||\mathbf{r}_i|| = x_i + y_i$ and $\mathbf{n}_i(\tau)$ is a slowly varying field that describes fluctuations around the corners of the original Brillouin zone, and the second slowly varying field $\mathbf{L}_i(\tau)$ describes fluctuations around $\mathbf{k}$=0, both being low-energy fluctuations; $\mathbf{L}_i(\tau)$ takes into account fluctuations of the local ferromagnetic spin density. The square-root normalization factor puts $\mathbf{n}_i(\tau)$ on the unit sphere. In the original Hamiltonian formulation of the model, the field $\mathbf{n}$ corresponds to the local expectation value of the staggered magnetization operator and $\mathbf{L}$ to the total spin in a small region of space containing a large number of microscopic degrees of freedom. Therefore, $\mathbf{L}$ is the generator of rotations in spin space and satisfies the constraint $\mathbf{L} \cdot \mathbf{n}$=0. Substituting (11) in the expression for the Berry phase, expanding about the Néel state, and keeping terms quadratic in $\mathbf{L}$ and $\nabla\mathbf{n}$, we obtain

$$S \sum_i (-1)^{||i||} \Sigma(\mathbf{r}_i) + \int d^d x \int_0^{\beta} d\tau (\mathbf{n} \cdot \partial_\tau \mathbf{n} \times \mathbf{L}) \, , \tag{12}$$

where $\Sigma(\mathbf{r})$ is the area covered by the unit vector $\mathbf{n}$ on the unit sphere during the entire Euclidean-time evolution. Furthermore, using (11) and (9) and keeping terms up to order $|\nabla n|^2$ and L^2 we obtain

$$H = \frac{1}{2} \int d^d r \left(\frac{|\mathbf{L}|^2}{\chi_{\perp}^0} + \rho_s^0 |\nabla \mathbf{n}|^2 \right) \, , \tag{13}$$

where $\chi_{\perp}^0$ and ρ_s^0 are the bare perpendicular susceptibility and spin-stiffness constant. These constants at the cutoff level are given by $\rho_s^0 = JS^2a^{2-d}$ and $\chi_{\perp}^0 = 1/4dJa^d$ and they are correct in the classical limit $S \rightarrow \infty$. The resulting action is quadratic in the field $\mathbf{L}$, which can be integrated out to yield the nonlinear σ model

$$Z = \int [D\mathbf{n}] \exp\left(-\frac{\rho_s^0}{2} \int_0^{\beta} d\tau \, d^d r (|\nabla \mathbf{n}|^2 + c_0^{-2} |\partial_\tau \mathbf{n}|^2) + i\Theta \right) \, , \tag{14}$$

where $c_0 = \sqrt{\rho_s^0/\chi_{\perp}^0} = 2\sqrt{d}SJa$ is the bare spin-wave velocity. Here Θ is the purely topological part of the Berry phase $\Theta = S\sum_i (-1)^{||i||} \Sigma(\mathbf{r}_i)$.

In one space dimension and in the continuum, the Berry phase can be interpreted as[5] $\Theta = (S/2) \int dx (\partial_x \Sigma)$, which is $S/2$ times the area of the unit sphere. Therefore, this phase distinguishes integer from half-integer spin chains. In the case of half-integer spin chains we have fermion (topological) excitations due to the Berry phase factor of $e^{i\pi}$. Hence, the continuum limit of the AF Heisenberg spin chain is a different field theory for integer and half-integer spins.

In 2+1 dimensions, assuming *smooth* configurations, the phase Θ can be interpreted as $\Theta = S\sum_y (-1)^y \Theta_y$, where $\Theta_y = \int dx \, \partial_x \Sigma(x, y, \tau)$. For a continuous field $\mathbf{n}(x, y, \tau)$, Θ_y is a continuous function of y, and, since it can only take integer multiples of 4π, it must be a constant. Therefore, assuming that only smooth configurations are important, Θ vanishes in 2+1 dimensions.

III. SMOOTHNESS OF CONFIGURATIONS

These arguments are based on the assumption that the Euclidean-time path of a spin degree of freedom in a typical multispin configuration from those that dominate the partition function are smooth, i.e., $\mathbf{n}_i(\tau)$ is a smooth function of τ. It is, therefore, interesting to study when the smoothness condition is satisfied in the model. In Ref. 9, the phase diagram and the continuum limit of the model (14), with $\Theta = 0$ and regularized on a (2+1)-dimensional lattice, was investigated. The action of the model is defined on the lattice with lattice spacing a as follows:

$$\mathbf{S} = -\frac{1}{2g} \sum_{\mathbf{x}} \sum_{\mu=1}^{3} \mathbf{n}(\mathbf{x}) \cdot [\mathbf{n}(\mathbf{x} + \hat{\mathbf{e}}_\mu) + \mathbf{n}(\mathbf{x} - \hat{\mathbf{e}}_\mu)] \, , \tag{15}$$

where $\mathbf{x}$ covers the (2+1)-dimensional space-time lattice of lattice spacing a and size $L^2 L_\beta$, i.e, $x_1, x_2 = 1, 2, ..., L$, $x_3 = 1, 2, ..., L_\beta$, and $\beta\hbar c_0 = L_\beta a$, $g = hc_0/\rho_0 a$. We impose periodic boundary conditions. In this model, the average of the field $\vec{n}$ is proportional to the average staggered magnetization of the model (1).

The phase diagram of the σ model in 2+1 dimensions is illustrated in Fig. 1. At $T = 0$, it has an ordered phase for $g < g_c = 1.45 \pm 0.01$, while at $T > 0$ the space-time reduces to a two-dimensional slab of thickness $\hbar c\beta$,

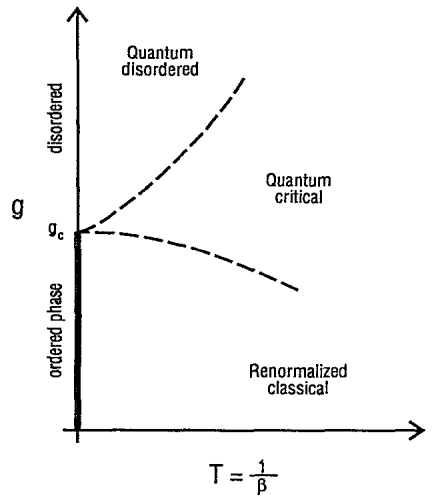

FIG. 1. The phase diagram of the nonlinear σ model in 2+1 dimensions. The value of g_c was determined in Ref. 9 to be $g_c = 1.45 \pm 0.01$. The dashed lines are crossover lines between regions where the correlation lengths assume different temperature dependence.

and the model has a disordered phase for all values of g. However, there are different regions of the parameter space that are separated by crossover lines. For example, for $g < g_c$ and as $T \to 0$, the correlation length is exponentially large, i.e.,

$$\xi(g < g_c, T \to 0) = Ce^{\frac{2\pi\rho_s}{kT}} , \tag{16}$$

and the elementary excitations of the system are spin waves that are well-defined excitations for wave numbers k larger than the inverse correlation length $[k\xi(T) >> 1]$. The model is believed[7,8] to behave as the classical 2D nonlinear σ model with a renormalized coupling constant g (or in terms of physical parameters, with a renormalized spin-stiffness constant ρ_s). This region is referred to as "renormalized classical regime." For $g > g_c$ and $T \to 0$, the model is characterized by disorder, and the correlation length is weakly temperature dependent and to a good degree of approximation is a constant of the order of the lattice spacing. In this phase the spin waves are not well-defined excitations, and the long-range order is destroyed even when switching off thermal fluctuations (T=0, i.e., infinite slab thickness). Since quantum fluctuations destroy the long-range order, this regime is called "quantum disordered region." For $g \sim g_c$ and $T \to 0$ the thermal fluctuations have a comparable effect to that of the quantum fluctuations, and the correlation length behaves as

$$\xi(g = g_c, T) = C' \frac{\hbar c}{kT} . \tag{17}$$

In Fig. 2, we give examples of configurations. The configuration given at the top left corner is obtained taking g=0.1, while the one on the top right corner is obtained with g=1.1 and the configuration at the bottom of the figure is obtained for g=1.45 (the critical point). We notice that for small values of g the configurations are of

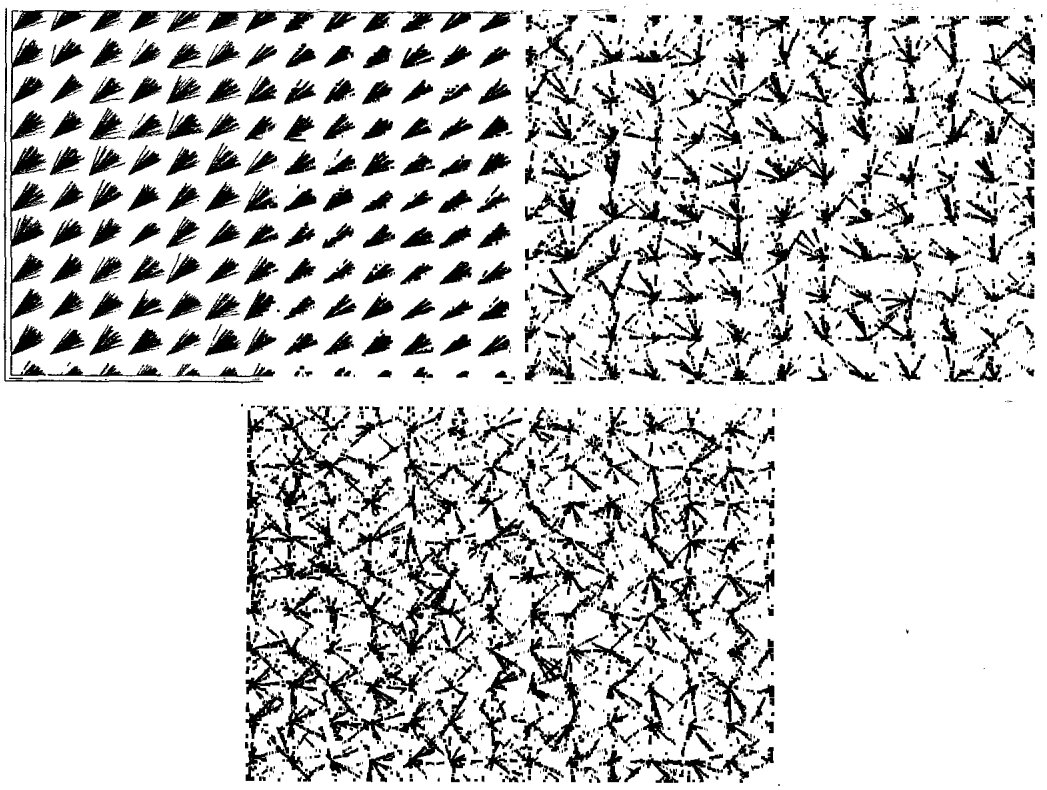

FIG. 2. Typical equilibrium configurations on a 32^3 size lattice. Each vertex represents a spatial site (x,y) and the lines emerging from the vertex are the directions of the spins during the 32 Euclidean time slices from 0 to β. Top left: The configuration is obtained at g=0.1. Top right: g=1.1. Bottom: g=1.45.

small amplitude as expected, and as the critical point is approached the configurations become less smooth because the value of the order parameter is reduced due to quantum fluctuations. In mapping the spin-S AF Heisenberg model onto the σ model, we found[3] that the $S = \frac{1}{2}$ case corresponds to approximately $g = 1.1$ when we take the lattice spacing unit in both models to be the same; the average staggered magnetization in both cases is reduced by the same amount (approximately 40%) from its classical saturated value due to quantum fluctuations.

The lack of smoothness in configurations obtained for g=1.1 is consistent with the behavior of the spin-spin correlation function calculated in Ref. 9. In Fig. 3 of Ref. 9, the spin-spin correlation function was shown for g=1.25 and for a $100^2 \times 6$ lattice. We notice that there is a long correlation length associated with the long-distance behavior of the correlation function (which becomes infinite in the T=0 limit), while the spin-spin correlation function for nearest-neighbor spins is reduced to 0.7 and for next-nearest neighbors to 0.55. Namely, the expectation that, due to the presence of the long correlation length, the directions of nearest-neighboring spins differ by a small amount is not correct. The situation becomes worse when we approach the critical point g_c, since the asymptotic value of the correlation function becomes even smaller; thus the value of the short-range correlation decreases further.

Smoothness can be achieved at any $g < g_c$ by means of real-space block-spin transformations. In Fig. 3, we present a configuration at a fixed Euclidean-time slice on a 32^3 lattice obtained at g=1.1 after thermalization starting from a random configuration. The value of the order parameter calculated on this configuration is 0.6195. In the inset of the figure we give the Euclidean-time evolution on the unit sphere of a spin located on this plane. The lack of smoothness is clear. In Fig. 4, we give the same time slice of a configuration on a 16^3 lattice obtained from the one of Fig. 3 after real-space block-spin transformation defined as follows: We calculate

$$\mathbf{n}'(i_x, i_y, i_z) = \sum_{\delta_x, \delta_y, \delta_z = 0,1} \mathbf{n}(i_x + \delta_x, i_y + \delta_y, i_z + \delta_z) , \tag{18}$$

and normalize it to unity. It is clear that after removing the short-range fluctuations by block-spin transformation the configuration is much smoother. The value of the order parameter for the new configuration is raised to 0.819. Notice that the spins point in an arbitrarily chosen direction, approximately defined by the diagonal of the x-y plane. The block-spin transformation can be repeated on the new configuration to obtain the ones of Fig. 5 on lattices of size 8^3 (left) and 4^3 (right). The value of the order parameter increases to 0.918 and 0.970, respectively, and thus the block-spin transformation corresponds to changing g to smaller values (higher-spin cases). The argument given by Haldane for the disappearance of the Berry phase is based on the assumption that the configurations are smooth at the level of the lattice spacing without blocking. For g=1.1, however, a typical configuration has the degree of smoothness possessed by the one of Fig. 3.

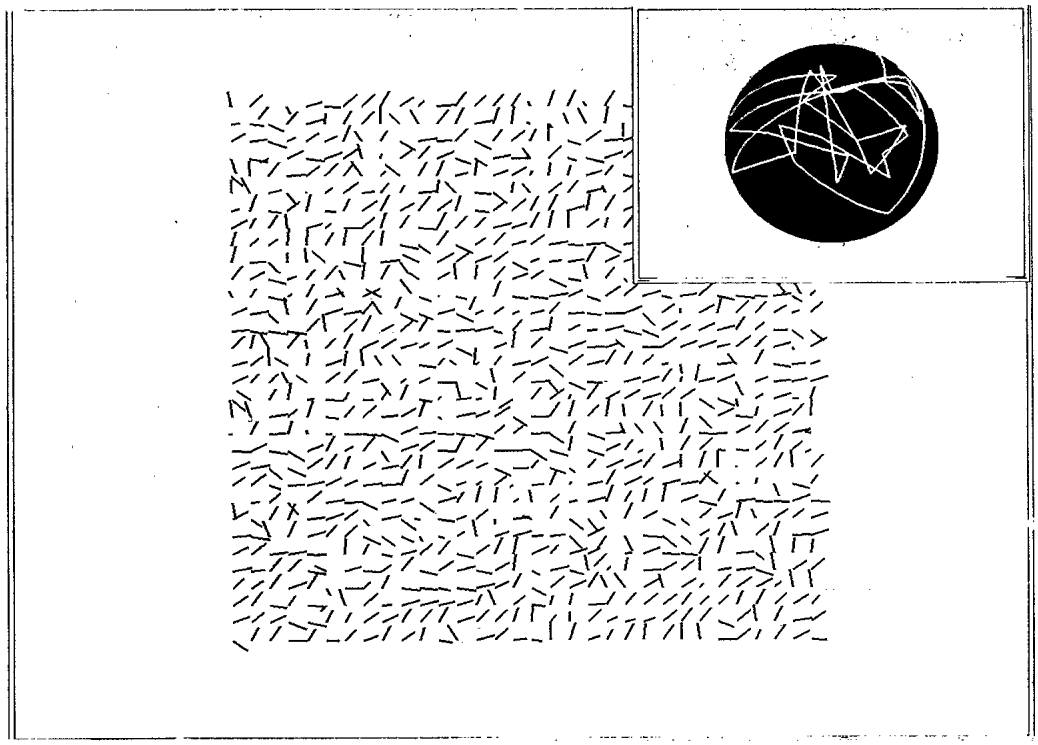

FIG. 3. Typical spin-configuration for a plane of fixed τ at g=1.1 (which corresponds to $S = \frac{1}{2}$ on the square lattice). The inset gives the trajectory on the unit sphere of a spin at site (x, y) of the plane during the Euclidean-time evolution.

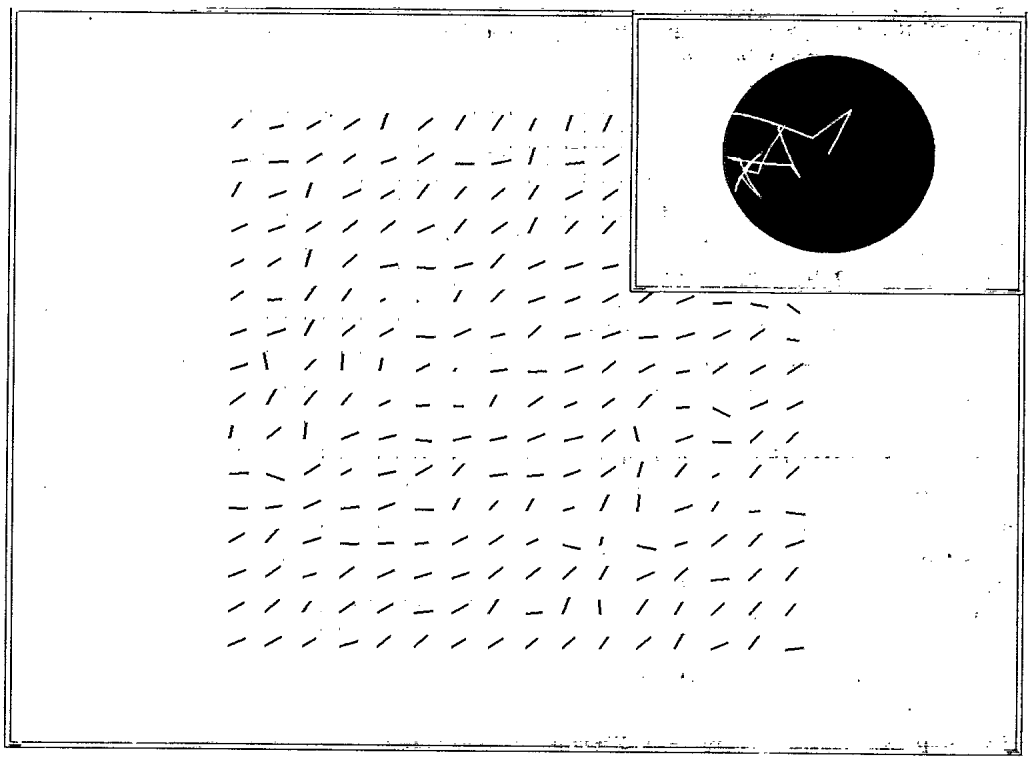

FIG. 4. The configuration of previous figure after one block-spin transformation defined by Eq. (18).

figurations are smooth at the level of the lattice spacing without blocking. For g=1.1, however, a typical configuration has the degree of smoothness possessed by the one of Fig. 3.

We wish to point out that we have observed smooth configurations dynamically generated as follows. For values of $g < g_c$, which correspond to the ordered phase, when we start from an initial random configuration using a local spin update it takes many thousands of configurations for thermalization. Typically after 50 000–100 000 sweeps through the entire lattice, the system chooses a certain direction for the average value of $\mathbf{n}$ to point. After a few thousand sweeps, however, the spin system can reach local equilibrium, but it is still far from the global equilibrium. In Fig. 6, we present a typical example of such configuration (a plane of fixed τ) and in the insets the Euclidean-time evolution of a spin at a given spatial site (x, y) is shown. It is clear from both figures that the configuration is smooth. It is easy to understand why such configurations can occur only under the above conditions; the spins are thermalized locally and they choose a certain direction to point that is differ-

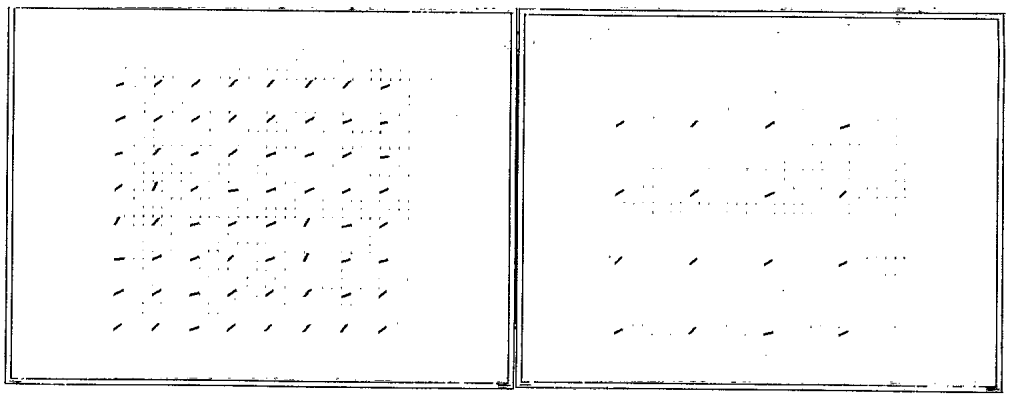

FIG. 5. The top left (right) figure presents the configuration obtained after two (three) consecutive block-spin transformations are applied on the configuration of Fig. 3.

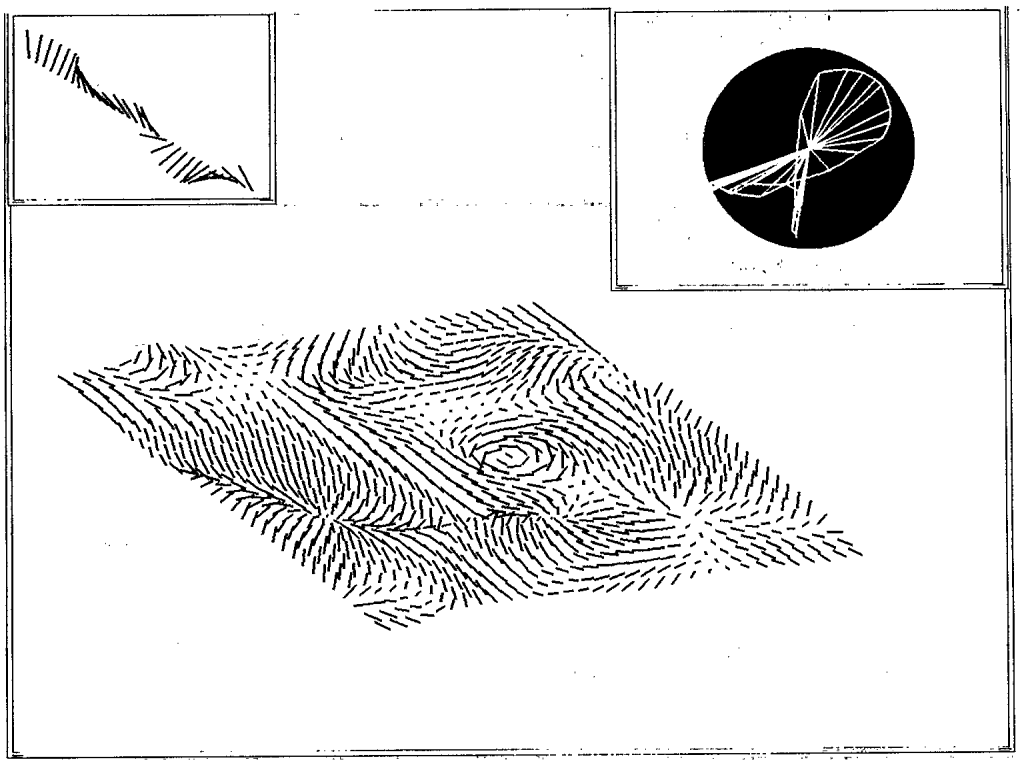

FIG. 6. Typical example of a nonequilibrium configuration at a plane of fixed τ in the ordered phase. In the right inset the Euclidean-time evolution on the unit sphere of a spin at a given spatial site (x, y) is shown. In the left inset the smoothness of the trajectory $\mathbf{n}_i(0), \mathbf{n}_i(\tau_1), \mathbf{n}_i(\tau_2), \ldots, \mathbf{n}_i(\tau_{L-1})$ of the spin at certain site i of the plane is illustrated.

ent for different regions of the lattice; there is no global direction because of the fact that the global thermalization time is longer. The directions of the spins located between the various regions (domains) of the lattice interpolate smoothly from one direction in one domain to the other as required to keep the free-energy low.

Another question that one might ask is whether the structures in such configurations are typical spin-wave configurations or whether they carry nontrivial topological-charge distribution. We shall attempt to answer such questions in the Sec. V.

IV. SOLID ANGLE CORRELATIONS

Shankar,[10] introduces static holes in the Heisenberg model and considers their imaginary time evolution. Imagine for example that we pull out a spin from site i at time τ_1 and replace it at time τ_2. Shankar keeps the σ model action as before, and subtracts the contribution that the spin at i would have made to the action. One important contribution is obtained just by taking out the Berry phase. Thus, the hole erases a contribution of the phase

$$\delta S = -iS(-1)^{||i||}\Sigma(\mathbf{r}_i) \ , \tag{19}$$

which is written in the following form:

$$\delta S = -iS(-1)^{||i||}\int_{\tau_1}^{\tau_2} d\tau\, a_0(i,\tau) \ , \tag{20}$$

$$a_0(i,\tau) = \mathbf{A}\cdot\frac{\partial \mathbf{n}}{\partial \tau} \ , \tag{21}$$

and is the same as a Wilson line in the path integral for the σ model. By introducing two such holes in the σ model, we can study their interference, and we can define the static potential as the energy of introducing two holes at τ=0, one at i and the second at j, and removing them at infinite time. Therefore,

$$e^{-\beta(V_{ij}+\text{const})} = C_{ij} \equiv \int [D\mathbf{n}] \exp\{-iS(-1)^{||i||}[\Sigma(\mathbf{r}_i) + (-1)^{||j-i||}\Sigma(\mathbf{r}_j)]\}$$
$$\times \exp\left(-\frac{\rho_s^0}{2}\int_0^\beta d\tau\, d^d r(|\nabla \mathbf{n}|^2 + c_0^{-2}|\partial_\tau \mathbf{n}|^2)\right) \ , \tag{22}$$

and we shall need to take the limit of $\beta \to \infty$. Notice that we have assumed that after adding the contribution of the spin to the Berry phase the Θ term is assumed zero.

There is, of course, a contribution to the hole-hole interaction due to the fact that the two static holes when they are next to each other break one less bond. We have eliminated this contribution in order to focus our attention on the contribution from the phase interference, as discussed in Ref. 10. We would like to remind the reader that in the copper oxide materials the hole-hopping matrix t is large compared to the energy scale J controlling spin excitations, and thus the static hole limit may not be realistic. It is instructive, however, to study whether there is a significant *contribution* to hole-hole interaction due to Berry phase coherence as argued in Ref. 10.

We calculated the area $\Sigma(\mathbf{r}_i)$ on the unit sphere defined by the path of the spin at $\mathbf{r}_i$ during the Euclidean-time evolution. For a given path there are two areas on the unit sphere adding up to 4π radians (the area of the entire sphere). We have followed the following convention: Consider the trajectory of the spin at the ith site, $\mathbf{n}_i(0), \mathbf{n}_i(\tau_1), \mathbf{n}_i(\tau_2), \ldots, \mathbf{n}_i(\tau_{L-1})$ with $0 < \tau_1 < \tau_2 < \cdots$ and $\mathbf{n}_i(\tau_L) = \mathbf{n}_i(0)$. We consider the spherical triangle defined by the north pole and the tips of the vectors $\mathbf{n}_i(\tau_{n-1})$ and $\mathbf{n}_i(\tau_n)$. The area of this triangle is considered positive (negative) if the point $\mathbf{n}_i$ (τ_n) is to the right (left) of the great circle passing through the north pole and the point $\mathbf{n}_i(\tau_{n-1})$. The total area is the sum of the areas of the spherical triangles with the above sign convention,

$$\Sigma(\mathbf{r}_i) = \sum_{l=1}^{L} T[\hat{z}, \mathbf{n}_i(\tau_l), \mathbf{n}_i(\tau_{l+1})] \ , \tag{23}$$

where $T(\mathbf{n}_1, \mathbf{n}_2, \mathbf{n}_3)$ is the exact expression for the area of a spherical triangle defined by the vertices $\mathbf{n}_1$, $\mathbf{n}_2$, and $\mathbf{n}_3$ on the surface of the unit sphere.

In Figs. 7(a) and 7(b), we present the results of our simulation of the correlation function $C_{ij} = \langle \exp\{iS[\Sigma(\mathbf{r}_i) + (-1)^{\|j-i\|}\Sigma(\mathbf{r}_j)]\}\rangle$ as a function of $r_{ij} = |\mathbf{r}_{ij}|$. Figure 7(a) [7(b)] gives C_{ij} calculated for g=1.1 with i, j in the same (opposite) sublattice. As explained earlier, the staggered magnetization at g=1.1 and T=0 is reduced to about 60% of its classical value, and it should correspond to the $S = \frac{1}{2}$ quantum AFHM on the square lattice. Notice that the correlation function attains its asymptotic value after a few lattice constants; in fact, as can be seen from the figure, the contribution to the hole-hole interaction due to this term is negligible beyond nearest neighbor. This is consistent with the findings of Ref. 9, where the size of the finite correlation length in the ordered phase (for values of g close to the above value) was found to be of the order of the lattice spacing. Note that there are two correlation lengths in the ordered phase of the σ model, a finite correlation length associated with the variation of the radial mode (σ mode) and (at T=0) an infinite correlation length associated with the correlations of the angular mode (π mode). We repeated the calculation of the correlation function C_{ij} for other values of g both in the ordered ($g < g_c$) and disordered phase ($g > g_c$) of the σ model. We found that the correlation function has qualitatively similar behavior to that shown in Fig. 7.

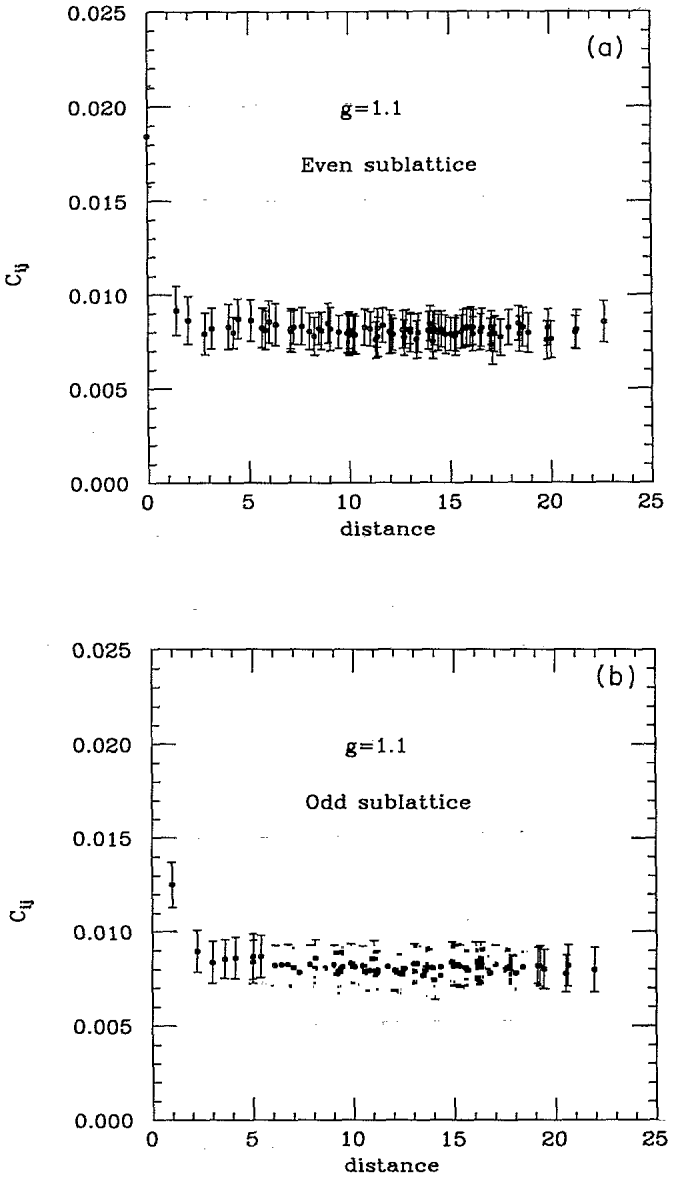

FIG. 7. The results of our simulation for the Berry-phase correlation function C_{ij} plotted as a function of $r_{ij} = |\mathbf{r}_{ij}|$. (a) C_{ij} calculated for g=1.1 with i, j in the same sublattice. (b) C_{ij} calculated for g=1.1 with i, j in opposite sublattices.

V. TOPOLOGICAL CHARGE OF THE CONFIGURATIONS

One more question that we wish to answer is whether or not the dynamically generated configurations such as those of Fig. 6 have a topological (monopole) charge distribution. Such configurations[11,12] are those that realize

the Hopf map $S^3 \rightarrow S^2$, where S^3 refers to the compactified Euclidean space time and S^2 the surface of the unit sphere of $\mathbf{n}$. To detect such structures in a given dynamically generated configuration such as the one presented in Fig. 6, we need the appropriate tools. Let us imagine a single monopole configuration located at the center $\tau = x = y = \frac{L}{2}$ of a L^3 lattice. Next, we create a rectangular loop parallel to the x-y plane, and we place it initially under the singularity as far away from it as possible; say its center is at τ=0, $x = y = \frac{L}{2}$. As we walk in a given sense, say counterclockwise, around the loop, the perimeter of the loop maps onto a loop on the unit sphere where the spin $\mathbf{n}$ resides. When the loop is far away from the monopole configuration, the area of the loop generated by the spin on the unit sphere is close to 4π (in fact for $L \rightarrow \infty$ it is exactly 4π). Imagine, now, that we move the loop forward in Euclidean time keeping it parallel to its original location so that its center is at $x = y = \frac{L}{2}$. The area of the loop on the unit sphere as a function of τ changes from 4π (at τ=0) to 0 (at $\tau = \infty$). We have used this test to see if there are topological charges in configurations like the one presented in Fig. 6, by placing the loop at several locations where one, by looking at the configuration, might suspect the presence of such singularities. This method may fail to detect the charges if there is a monopole and antimonopole pair close to each other and the size of the loop is larger than their separation distance. We changed the size and the initial location of the loop to avoid this problem. We concluded that the configurations are free of such singularities.

Huang, Koike, and Polonyi (HKP) have recently suggested[13] that the phase transition in the nonlinear σ model as a function of g should not be understood as a conventional order-disorder transition,[7-9] but rather as a transition triggered by such topological configurations. They calculated the density of such configurations approximately by examining whether or not the eight spins on the vertices of an elementary cube of a size equal to the lattice spacing cover the surface of the unit sphere. However, because of short-range fluctuations (as is clear from Fig. 2), the spins in a typical eight-spin configuration in the disordered phase, point in different directions in such a way that the approximate algorithm used by HKP to incorrectly detect presence of a monopole. The monopole configuration is a long-range structure and cannot be accurately detected by looking at such small sized cubes. Using the definition used by HKP, we calculated the monopole density of a randomly generated configuration, and we found that it is in the range of values obtained by HKP (shown in their Fig. 6) in the disordered phase.

The conclusion of this section is that we have not been able to find any indication that topological monopole configurations play an important role in the dynamics of this model. Furthermore, to calculate the monopole density on the lattice one needs to search for long-range structures because of the presence of short-range fluctuations. Monopole configurations are long-range excitations and it costs finite energy on the lattice to create short-range fluctuations that might be counted as monopoles in a simple definition of the monopole density using the spins of elementary cubes.

VI. CONCLUSIONS

The nonlinear σ model in 2+1 dimensions, because of its possible relevance to the physics of the copper oxide superconductors, is recently under theoretical investigation. Using the Monte Carlo method, we have studied the nature of the configurations in the model as well as Berry-phase correlations because, as suggested in Refs. 10 and 15, it might give rise to attraction between holes when introduced in a quantum antiferromagnet.

We find that the configurations contributing to the partition function are not smooth for the case that corresponds to the spin-$\frac{1}{2}$ AFHM on the square lattice. Such configurations become smooth after block-spin transformation, which reveals the long-distance behavior. The derivation of the QNLσM from the spin-$\frac{1}{2}$ AFHM requires that the important configurations be smooth without blocking of the spins, i.e., smooth at the cutoff level. For instance, the Hopf term that distinguishes the half-integer from the integer-spin case vanishes, if moving from one space-time plane to the nearest-neighboring one the configurations change by a small amount.[6] However, the QNLσM can be also introduced as the long-wavelength low-energy limit of the Heisenberg antiferromagnet in a different way using arguments based on the symmetry of the order parameter (staggered magnetization). As long as the continuous O(3) symmetry is spontaneously broken, the interaction of the Goldstone modes of the system in the long-wavelength limit can be described by this model regardless of the details of the microscopic Hamiltonian and the value of the spin.[14]

Motivated by the work of Shankar[10] and that of Lee[15] we have calculated the Berry-phase correlation function defined by Eq. (22); this correlation function gives the contribution to the hole-hole interaction due to Berry-phase constructive interference in the path integral over all possible spin configurations. Our results indicate that the correlation function attains its asymptotic value within a few lattice spacings. In addition, we found no sign change in the interaction when the holes are on the same or opposite sublattices in disagreement with the expectations of Ref. 10. Thus, our calculation here indicates that the *contribution* to hole-hole interaction due to the mechanism suggested in Ref. 10 is not significant beyond nearest neighbors. Shankar's suggestion was based on what happens in the (1+1)-dimensional case where a dynamically generated gauge field couples to the hole motion and becomes responsible for the hole-hole attraction; our numerical results indicate that the situation may be different in 2+1 dimensions, which is the case of interest and applicable to the cuprous oxides. These

results by no means indicate lack of significant hole-hole attraction in quantum antiferromagnets. We believe that there may be attraction between *mobile* holes in such systems as a result of the antiferromagnetic correlations. In fact, the results of Ref. 16 show that there is tendency for hole-pairing in a certain range of the parameters of the strong-coupling Hubbard model using exact numerical diagonalization of small-size clusters.

Finally, we studied the existence of monopole charge in certain configurations featuring smoothness, and we found zero topological charge. Instead, such smooth configurations are dominated by large-amplitude spin waves. Thus, our results are consistent with the expectation that spin-wave excitations are the low-lying excitations at low temperatures.

ACKNOWLEDGMENTS

We would like to thank R. Shankar for useful discussions; the calculation of Sec. IV was mainly encouraged by his interest in the results of such a calculation. We wish to thank E. Pepke for his assistance and for using his color graphics routines to represent the paths of the spins on the unit sphere during their Euclidean-time evolution. This work was supported in part by the Supercomputer Computations Research Institute, which is partially supported by the U.S. Department of Energy under Contract No. DE-FC05-85ER-250000 and by the U.S. Defense Advanced Research Projects Agency (DARPA) sponsored Florida Initiative for Microelectronics and Materials under Contract No. MDA972-88-J-1006.

[1] Y. Endoh *et al.*, Phys. Rev. B **37**, 7443 (1988).
[2] H. Monien, P. Monthoux, and D. Pines (unpublished); F. Mila and T. M. Rice, Physica C **157**, 561.
[3] E. Manousakis, Rev. Mod. Phys. (to be published).
[4] F. C. Zhang and T. M. Rice, Phys. Rev. B **37**, 3759 (1988).
[5] F. D. M. Haldane, Phys. Rev. Lett. **50**, 1153 (1983); I. Affleck, Nucl. Phys. **B257**, 397 (1985).
[6] F. D. M. Haldane, Phys. Rev. Lett. **61**, 1029 (1988).
[7] S. Chakravarty, B. I. Halperin, and D. Nelson, Phys. Rev. Lett. **60**, 1057 (1988).
[8] S. Chakravarty, B. I. Halperin, and D. Nelson, Phys. Rev. B **39**, 2344 (1989).
[9] E. Manousakis and R. Salvador, Phys. Rev. Lett. **61**, 1310 (1989); Phys. Rev. B **40**, 2205 (1989).
[10] R. Shankar, Phys. Rev. Lett. **63**, 203 (1989).
[11] F. Wilzcek and A. Zee, Phys. Rev. Lett. **51**, 2250 (1983).
[12] A. M. Polyakov, Mod. Phys. Lett. (Singapore) A **3**, 325 (1988).
[13] K. Huang, Y. Koike, and J. Polonyi (unpublished).
[14] B. Rosenstein, B. J. Warr, and S. H. Park, Nucl. Phys. **B336**, 435 (1990).
[15] P. A. Lee, Phys. Rev. Lett. **63**, 680 (1989).
[16] E. Kaxiras and E. Manousakis, Phys. Rev. B **38**, 866 (1988); J. A. Riera and A. P. Young, *ibid.* **39**, 9697 (1989).